

# Gradient Unwarping for Phase Imaging Reconstruction

Paul Polak<sup>1</sup>, Robert Zivadinov<sup>1,2</sup>, and Ferdinand Schweser<sup>1,2</sup>

<sup>1</sup>Department of Neurology, Buffalo Neuroimaging Analysis Center, State University of New York at Buffalo, Buffalo, NY, United States, <sup>2</sup>Molecular and Translational Imaging Center, MRI Center, Clinical and Translational Research Center, Buffalo, NY, United States

**TARGET AUDIENCE:** Researchers interested in quantitative phase imaging and reducing co-registration artifacts.

**INTRODUCTION:** Gradient non-linearities result in spatial displacement of the imaging voxel signal (distortions) when the acquired  $k$ -space data is reconstructed by direct Fourier transform. Deviations from linearity are generally minimal at iso-center, but are always present and increase with distance. Consequently, the image distortion depends on the position of the subject in the scanner as well as the location and orientation of the imaging slab. The overall severity of the distortion depends on the extent of the subject's anatomy, for example the size of the subject's head. Distortion is particularly evident in abdominal imaging, but also poses problems for neuroanatomy. Correction of the gradient warp [1], also referred to as *gradient unwarping*, is an important step for certain quantitative metrics; e.g., volumetric measurements of neuroanatomy. If warping is not corrected in this case, study outcomes would be highly biased by the head size.

Gradient unwarping is typically applied as a black-box slice-wise (2D) post-processing step to magnitude images at or near the end of the manufacturer's image reconstruction pipeline, after the multi-channel image combination. However, in a research environment, imaging data is often taken at a more primary step, such as raw  $k$ -space data or uncombined single channel data. Although this data are generally warped they represent the basis of many novel sophisticated image reconstruction techniques that are currently subject to clinical exploration, such as non-Cartesian image reconstruction, compressed sensing, or multi-channel phase image reconstruction, e.g., in the course of quantitative susceptibility mapping (QSM). In any of these cases, it is the researcher's responsibility to unwarp the images. Gradient unwarping avoids bias and is essential for a comparison of research sequences to (unwarped) images directly obtained from the scanner's reconstruction system, e.g. T<sub>1</sub>-weighted (T<sub>1</sub>w) DICOM images that are commonly used as a basis for image segmentation. However, to the best of our knowledge, gradient unwarping is usually neglected in the MR image reconstruction community. We present here a method to properly unwarp complex-valued MRI data and demonstrate the importance of gradient unwarping as a processing step in the framework of QSM, although the methodology is applicable also to other phase-sensitive reconstruction techniques.

**THEORY AND METHODS:** The theory of gradient unwarping was described in Refs. 2 and 3. However, in contrast to magnitude images, phase images cannot be unwrapped directly as they are non-continuous (phase wraps), presenting obvious problems with the involved spatial interpolation. To unwarp complex-valued data we propose to separately unwarp real and imaginary parts of the complex-valued images and, finally, calculate magnitude and phase from the resulting images. We present here an algorithm for 2D or 3D gradient unwarping. Our algorithmic development is based on the code provided at <https://code.google.com/p/gradunwarp/> [2]. Specifically, this code was extended to allow for an arbitrary specification of the gradient displacement field and modified to be able to handle negative image intensities, which is required to unwarp real and imaginary images of data with a phase component. The method was validated in a structure phantom (**Figure 1**) and applied to a database of 1400 clinical 3D fully flow-compensated GRE datasets. All data were acquired with a multi-channel head and neck coil on a 3 Tesla GE Signa Excite HD 12.0 (General Electric, Milwaukee, WI). Parameters of the clinical GRE sequence were: 512x256x64 matrix, 25.6 cm field of view (FOV) and 75% phase FOV, resulting in 0.5x0.75x2mm<sup>3</sup> voxel size, 12° flip angle, TE/TR 22ms/40ms. The gradient displacement field was calculated based on the scanner's gradient coil calibration file, available on the MRI system and used by the scanner's internal unwarping procedure. Single-channel real- and imaginary

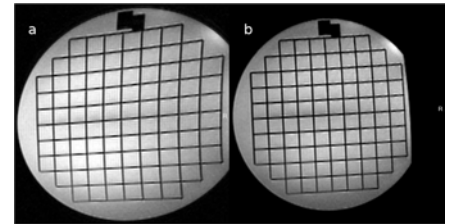


**Figure 1:** Warped (a; raw data) and unwrapped (b; with the algorithm presented in this contribution) axial images from a cylindrical phantom with a rectangular grid pattern.

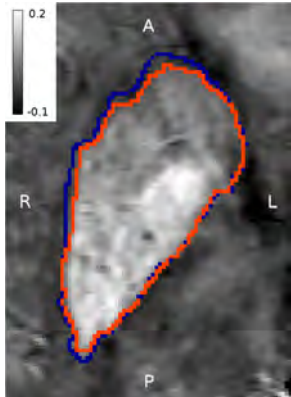


**Figure 2:** Section of an unwrapped axial susceptibility map showing the diencephalon. ROIs were drawn on the warped (blue) and unwrapped images (red). (scale in ppm)

areas with very different susceptibility values. For example, the diamagnetic internal capsule is adjacent to the paramagnetic globus pallidus. On the other hand, if nuclei are defined directly on the warped images, volume estimates, e.g., to quantify tissue atrophy, are biased by head size.

**CONCLUSION:** We recommend incorporation of gradient unwarping into image reconstruction frameworks that rely on raw (warped) MR data, such as phase reconstruction in the course of QSM. We will make our algorithm freely available to the research community.

**REFERENCES:** [1] Markl, M., et al. (2003). *Magn. Reson. Med*, 50(4):791–801. [2] Jovicich, J., et al. (2006). *NeuroImage*, 30(2):436–443. [3] Langlois, S., et al. (1999). *Magn. Reson. Imaging*, 9:821–831. [4] Patenaude, B., et al. (2011). *NeuroImage*, 56(3):907–922, 2011. [5] Hammond, K. E., et al. (2008) *NeuroImage*, 39(4):1682–1692. [6] Schweser F., et al. (2011). *NeuroImage*, 54(4):2789–2807. [7] Schweser, F. et al. (2012). *NeuroImage*, 62(3):2083–2100.

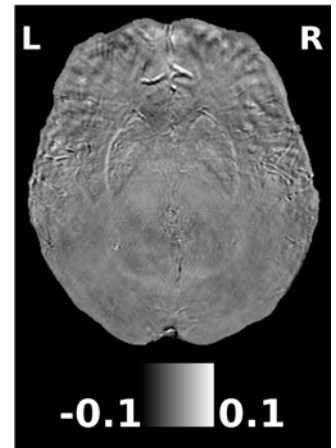


**Figure 3:** Difference image between warped and unwrapped QSM reconstructions (contrast range: -0.1 to 0.1 ppm). Noticeable differences are evident around anterior venous structures and diencephalon.